Rangeland Ecol Manage 67:563–572 | September 2014 | DOI: 10.2111/REM-D-13-00044.1

Utilizing National Agriculture Imagery Program Data to Estimate Tree Cover and Biomass of Piñon and Juniper Woodlands

April Hulet,[1] Bruce A. Roundy,[2] Steven L. Petersen,[3] Stephen C. Bunting,[4] Ryan R. Jensen,[5] and Darrell B. Roundy[6]

Authors are [1]Research Ecologist (postdoctorate), US Department of Agriculture–Agricultural Research Service, Eastern Oregon Agricultural Research Center, Burns, OR 97720, USA; [2]Professor, [3]Associate Professor, and [6]Graduate Student, Brigham Young University, Department of Plant and Wildlife Sciences, Provo, UT 84602, USA; [4]Professor, University of Idaho, Department of Forest, Rangeland and Fire Sciences, Moscow, ID 83844, USA; and [5]Associate Professor, Brigham Young University, Department of Geography, Provo, UT 84602, USA.

Abstract

With the encroachment of piñon (*Pinus* ssp.) and juniper (*Juniperus* ssp.) woodlands onto sagebrush steppe rangelands, there is an increasing interest in rapid, accurate, and inexpensive quantification methods to estimate tree canopy cover and aboveground biomass. The objectives of this study were 1) to evaluate the relationship and agreement of piñon and juniper (P-J) canopy cover estimates, using object-based image analysis (OBIA) techniques and National Agriculture Imagery Program (NAIP, 1-m pixel resolution) imagery with ground measurements, and 2) to investigate the relationship between remotely-sensed P-J canopy cover and ground-measured aboveground biomass. For the OBIA, we used eCognition® Developer 8.8 software to extract tree canopy cover from NAIP imagery across 12 P-J woodlands within the Sagebrush Steppe Treatment Evaluation Project (SageSTEP) network. The P-J woodlands were categorized based on the dominant tree species found at the individual sites for the analysis (western juniper, Utah juniper, and mixed P-J community). Following tree canopy cover extractions, relationships were assessed between remotely-sensed canopy cover and ground-measured aboveground biomass. Our OBIA estimates for P-J canopy cover were highly correlated with ground-measured tree canopy cover (averaged across all regions $r=0.92$). However, differences between methods occurred for western and Utah juniper sites ($P<0.05$), and were more prominent where tree canopy cover was $>40\%$. There were high degrees of correlation between predicted aboveground biomass estimates with the use of remotely-sensed tree canopy cover and ground-measured aboveground biomass (averaged across all regions $r=0.89$). Our results suggest that OBIA methods combined with NAIP imagery can provide land managers with quantitative data that can be used to evaluate P-J woodland cover and aboveground biomass rapidly, on broad scales. Although some accuracy and precision may be lost when utilizing aerial imagery to identify P-J canopy cover and aboveground biomass, it is a reasonable alternative to ground monitoring and inventory practices.

Key Words: remote sensing, object-based image analysis, biomass, *Pinus*, *Juniperus*, eCognition® Developer

INTRODUCTION

The expansion of piñon (*Pinus* ssp.) and juniper (*Juniperus* ssp.) woodlands across the western United States has increased considerably over the last century (Miller and Tausch 2001; Miller et al. 2005). As piñon and juniper (P-J) woodlands expand and increase in density, the productivity and diversity of shrub-steppe ecosystems diminishes (Miller et al. 2000; Bates et al. 2005), and bare ground increases, potentially accelerating soil erosion and runoff (Pierson et al. 2010). To effectively manage landscapes of these encroached woodlands and obtain the greatest economic and ecological benefits, it is crucial to identify P-J woodland developmental phase and current canopy cover (Miller et al. 2005; Davies et al. 2010; Miller et al. 2014; Roundy et al. 2014a, 2014b).

With the expansion of P-J woodlands, there has been a subsequent greater need for more rapid, accurate, and inexpensive quantification methods for estimating P-J canopy cover over large land areas. Additionally, the quantification of biomass at the landscape scale is also needed to prioritize fuel management strategies, predict fire behavior, and calculate carbon fluxes (Strand et al. 2008; Huang et al. 2009; Chuvieco et al. 2010; McGinnis et al. 2010). The ability to measure biomass of the dominant species can contribute to a better understanding of resource allocation such as the use of water resources and nutrients (Miller et al. 1987; Roundy et al. 2014b), and the potential use of P-J woodlands for biofuel (Skog et al. 2009).

Multiple studies have been conducted, using various remote-sensing platforms to estimate tree canopy cover. Juniper cover estimates from satellite imagery combined with light detection and ranging (lidar) data, for example, have been shown to be significantly correlated with field-based cover measurements (Sankey and Glenn 2011). Panchromatic and color aerial photographs have also been used to successfully classify P-J canopy cover using unsupervised and supervised classification methods (Anderson and Cobb 2004), and object-oriented

This is Contribution Number 17 of the Sagebrush Steppe Treatment Evaluation Project (SageSTEP), funded by the US Joint Fire Science Program, the Bureau of Land Management, the National Interagency Fire Center, the Great Northern Landscape Conservation Cooperative, and Brigham Young University.

Correspondence: April Hulet, US Dept of Agriculture–Agricultural Research Service, Eastern Oregon Agricultural Research Center, Burns, OR 97720, USA. Email: april.hulet@oregonstate.edu

Manuscript received 5 March 2013; manuscript accepted 11 June 2014.

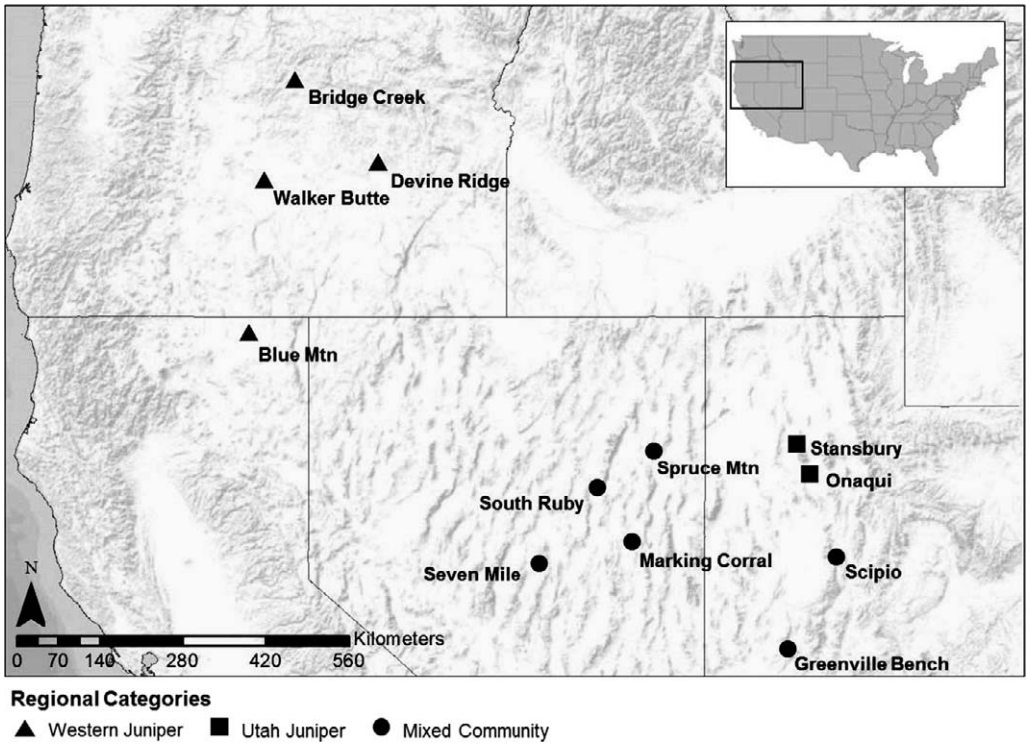

Figure 1. Study site locations across the Great Basin overlaid on imagery obtained from ArcGIS® online basemap gallery. Regional categories represent the dominant tree species found at the site, which include western juniper, Utah juniper, or a mixed community comprised of either singleleaf piñon or twoneedle piñon with Utah juniper.

classification methods (Weisberg et al. 2007; Ko et al. 2009; Davies et al. 2010; Madsen et al. 2011; Hulet et al. 2013, 2014). Few studies, however, have utilized remote sensing to estimate P-J aboveground biomass (Huang et al. 2009; Sankey et al. 2013).

The first objective of this study was to evaluate the relationship and agreement of P-J canopy cover estimates, using the National Agriculture Imagery Program (NAIP) imagery and object-based image analysis (OBIA) methods with ground-measured tree canopy cover. NAIP imagery is freely accessible and covers a wide range of areas potentially providing both researchers and land managers with opportunities to assess large landscapes spatially. OBIA methods, which allow users to create rule sets to classify image objects into meaningful land cover classes, were chosen for the image classification because of the increasing evidence that OBIA improves classification accuracy when compared to pixel-based classification methods (Platt and Rapoza 2008; Blaschke 2010; Meneguzzo et al. 2013). We hypothesize that NAIP imagery and OBIA methods are sufficient to extract tree canopy cover and would fall within an acceptable error rate when compared to ground measurements of tree canopy cover.

The second objective of the study was to evaluate the impact of spatial resolution on estimating P-J canopy cover. To assess the impact of spatial resolution, P-J canopy cover was extracted from high-resolution color imagery (0.06-m pixel resolution) and compared to P-J canopy cover extracted from NAIP imagery (1-m pixel resolution) using OBIA methods. We hypothesize the P-J canopy cover extracted from NAIP imagery would not be different from P-J canopy cover extracted using high-resolution imagery.

The third objective of the study was to investigate the relationship between predicted aboveground biomass estimates using remotely-sensed P-J canopy cover with ground-measured P-J aboveground biomass. Multiple field studies have found strong linear relationships between individual tree canopy cover and aboveground biomass (Miller et al. 1981; Tausch and Tueller 1990; Sabin 2008; Ansley et al. 2012). Hence, we hypothesize that the correlation between predicted and ground-measured aboveground biomass would be strong and sufficient to evaluate a landscape rapidly and prioritize management practices in P-J woodlands.

METHODS

Study Sites

Our study area included 12 SageSTEP P-J woodland sites found in Oregon, California, Nevada, and Utah (Fig. 1). Sites were placed in three regional categories depending on the dominant tree species found at the site including 1) western juniper (*Juniperus occidentalis* Hook.; JUOC); 2) Utah juniper (*Juniperus osteosperma* [Torr.] Little; JUOS); or 3) mixed community comprised of either singleleaf piñon (*Pinus monophylla* Torr. & Frém.) or twoneedle piñon (*Pinus edulis* Engelm.) with Utah juniper. Dominant shrub species by site included mountain big sagebrush (*Artemisia tridentata* Nutt. subsp. *vaseyana* [Rydb.] Beetle) at Blue Mountain, Devine Ridge, Walker Butte, and Stansbury; Wyoming big sagebrush (*Artemisia tridentata* Nutt. subsp. *wyomingensis* Beetle & Young) at Greenville Bench, Onaqui, Scipio, Marking Corral, Seven Mile, South Ruby, and Spruce Mountain; basin big

sagebrush (*Artemisia tridentata* Nutt. subsp. *tridentata*) at Bridge Creek; antelope bitterbrush (*Purshia tridentata* [Pursh] DC.) at Stansbury and South Ruby; and curl-leaf mountain mahogany (*Cercocarpus ledifolius* Nutt.) at Spruce Mountain, Blue Mountain, and Devine Ridge. Site characteristics have been further described by McIver and Brunson (2014).

At each site, fuel reduction treatment plots (2.5–24 hectares) were established across the range of P-J woodland successional stages (Miller et al. 2005; McIver et al. 2010), with tree canopy cover ranging from $< 5\%$ to $> 40\%$. Prior to treatments, 0.1 ha (33×30 m) subplots were randomly distributed throughout each plot. The number of subplots per site varied because of the total area and number of treatments at each site (McIver and Brunson 2014). For our study, pretreatment data (collected in 2006 and 2007) were used for 44 subplots at Bridge Creek, 43 at Devine Ridge, 46 at Walker Butte, 47 at Blue Mountain, 31 at Spruce Mountain, 42 at South Ruby, 44 at Seven Mile, 43 at Marking Corral, 60 at Stansbury, 69 at Onaqui, 56 at Scipio, and 60 at Greenville Bench.

Ground-Measured Data

P-J canopy cover by subplot was estimated by counting every tree that was greater than 0.5 m in height, and had the base of the trunk at least half-way within the established subplot. Tree clustering, or an overlap of branches between neighboring trees was minimal in the study; however, where it occurred overlapping branches were identified and included in the tree measurements. For each tree, the longest canopy diameter (or maximum foliage spread; *Dia1*) and the diameter perpendicular to the longest diameter (*Dia2*) were measured and used to calculate the crown area (A), using the following equation:

$$A = \pi/4(Dia1 * Dia2) \quad [1]$$

Percent tree canopy cover for each subplot was calculated by dividing the total tree crown area for the subplot by the total area of the subplot.

P-J biomass was also measured and calculated for every tree greater than 0.5 m in height, and had the base of the trunk at least halfway within the established subplot. Individual-tree aboveground biomass was estimated from allometric equations developed by Tausch (2009) as follows:

$$B_x = U_x V_x = U_x \pi/6\left(\left[C^2 H\right] - \left[\{C - 2F_x\}^2 * \{H - F_x\}\right]\right), \quad [2]$$

where $C > 2F_x$ and $H > F_x$, otherwise, $B_x = U_x V_x = U_x\ \pi/6C^2H$, where B_x is the total tree biomass, U_x is the tree bulk density, V_x is the total volume minus the volume without foliage, C is the two-canopy diameter measurements described above, H is the crown height of the tree, and F_x is the functional depth or foliage biomass distribution in a tree crown and the geometric relationship between the branch orders supporting that distribution. Total individual tree aboveground biomass was summed for each subplot and converted to kilograms per hectare.

Imagery Acquisition

Digital ortho quarter quad tiles (DOQQs) of the study sites were acquired from NAIP imagery (US Department of Agriculture 2008). All images were collected in 2006 with two exceptions: images from 2005 were used for Bridge Creek, and 2010 images were used for one plot at Marking Corral due to cloud obstruction in 2006. All DOQQs have a 1-m spatial resolution with the exception of Devine Ridge and Blue Mountain, which have a 0.5-m spatial resolution. The spectral bands used in our analysis were red (R), green (G), and blue (B) for all sites. In addition to NAIP RGB imagery, high-resolution RGB images (0.06-m pixel resolution) were used where data were available to evaluate the impact of spatial resolution on estimating P-J canopy cover, using OBIA methods. The high-resolution imagery was collected in 2009 with a Vexcel UltraCam X digital aerial camera (Vexcel Imaging GmBH, Graz, Austria) on board a turbocharged Cessna 206 aircraft. The camera was equipped with airborne GPS capabilities and Applanix inertial measurement units (IMU) that were supported by US Continuously Operating Reference Station/International Global Navigation Satellite System Service stations or dedicated GPS base stations at regional airports within the project area. Ground data were used to postprocess the airborne GPS/IMU data to yield air point coordinates for each exposure accurate to within ± 0.06 m. An image-to-image registration was used to position the high-resolution and NAIP imagery to one another for each site; the spatial accuracy of the data were determined to be acceptable when the RMSE < 0.5. The 3-yr difference between ground measurements and high-resolution imagery acquisition is considered to be minimal for tree canopy cover.

Image Processing

UTM coordinates of the four corners of each established 0.1 ha subplot were recorded, using a Trimble® GeoXT global positioning system (GPS) unit (Trimble Navigation Limited, Sunnyvale, CA). All points were differentially corrected with the use of GPS Pathfinder® Office software (Trimble Navigation Limited). Points were used to extract individual subplots from the landscape scene so measurements would be made on the same experimental unit for both OBIA and ground-measured tree canopy cover and aboveground biomass.

For each site, subplots were divided into two groups: training or validation. The training subplots (approximately 20% of the total subplots) were used to develop rule sets to classify P-J canopy cover, and to develop regression equations for estimating P-J aboveground biomass as explained below. Training subplots were selected to best represent the area of interest for classifying P-J canopy cover. For example, training subplots included varying ranges of tree canopy cover, varying amounts of shadows found within the imagery, and/or varying brightness values that were influenced by understory vegetation (e.g., antelope bitterbrush) or bare ground. Once rule sets and regression equations were developed from the training subplots, they were applied to the validation subplots (approximately 80% of the total number of subplots) for the statistical analysis.

To estimate P-J tree canopy cover from NAIP imagery, we used eCognition® Developer 8.8 software (Trimble Germany GmbH, Munich, Germany). The eCognition Developer software is an object-based image analysis (OBIA) software package that allows the user to develop rule sets to classify objects of interest. Our rule set distinguished two classes within each image: 1) a

Table 1. Regression statistics and coefficients for the relationship between the National Agriculture Imagery Program (NAIP) estimated piñon–juniper (P-J) cover and ground-measured P-J aboveground biomass for the training subplots by site. Equations developed were then used to predict P-J aboveground biomass of validation subplots.[1]

Sites	Model *P* value	*N*	Slope (SE)	Slope *P* value	Intercept (SE)	Intercept *P* value	Coefficient of determination
Devine Ridge	0.0057	9	763.22 (194.45)	0.0057	5 319.78 (5 212.39)	0.3414	0.6876
Walker Butte	< 0.0001	9	1 457.45 (103.75)	< 0.0001	−2 631.85 (1 304.94)	0.0835	0.9657
Bridge Creek	0.0034	8	527.99 (112.82)	0.0034	4 124.60 (2 144.23)	0.1028	0.7850
Blue Mountain	< 0.0001	9	1 174.33 (131.24)	< 0.0001	−3 370.13 (4 256.08)	0.4544	0.9196
South Ruby	0.0004	8	969.87 (135.09)	0.0004	3 704.90 (5 453.81)	0.5223	0.8957
Spruce Mountain	0.4036	4	633.10 (602.46)	0.4036	1 401.66 (17 262)	0.9427	0.3557
Marking Corral	0.0006	8	860.79 (133.02)	0.0006	−2 778.69 (4 290.17)	0.5412	0.8747
Seven Mile	< 0.0001	9	876.97 (83.10)	< 0.0001	1 956.30 (2 753.69)	0.5004	0.9409
Stansbury	0.0702	4	642.96 (179.96)	0.0702	−1 679.51 (4 973.49)	0.7677	0.8645
Onaqui	< 0.0001	12	708.49 (58.33)	< 0.0001	−1 71.07 (955.94)	0.8615	0.9365
Scipio	< 0.0001	12	824.98 (126.88)	< 0.0001	515.66 (3 047.18)	0.869	0.8087
Greenville Bench	< 0.0001	12	660.62 (53.36)	< 0.0001	1 430.15 (1 305.68)	0.2991	0.9388

[1]SE indicates standard error; *N*, number of subplots used to develop regression equations.

tree class, which consisted of piñon and juniper trees or clusters of trees, and 2) a nontree class, which included all other vegetation types, litter, bare ground, and shadow.

We used a multiresolution segmentation algorithm (Baatz and Schäpe 2000) to create image objects initially. Based on visual assessments of the image objects, we also applied a spectral difference algorithm that increased the median scale of image objects from 1.3 m^2 to 3 m^2. The spectral difference algorithm ultimately reduced the complexity of our image objects by merging neighboring image objects according to their mean image layer intensity values (Trimble 2011).

Once segmentation was complete, brightness values combined with the relative border feature (contextual feature that allows the user to grow or shrink objects based on neighboring image objects) were used to classify P-J canopy cover. Thresholds associated with each feature (brightness or relative border) were determined on a site-by-site basis with the use of training subplots. Once thresholds for each feature were developed, the rule set was applied to the validation subplots. The percentage of remotely-sensed tree canopy cover was then estimated for each of the validation subplots by first extracting the area of each polygon that represented the tree class, and then dividing tree class area by the total area of the subplot.

Predicted Aboveground Biomass

P-J aboveground biomass was also estimated on a site-by-site basis. A linear regression was created, using remotely-sensed tree canopy cover estimates from the training subplots on ground-measured aboveground biomass estimates (Table 1). The regression equations developed for each site were then applied to the validation subplots, using the remotely-sensed tree canopy cover estimates (explanatory variable) to predict P-J aboveground biomass (dependent variable).

Accuracy Assessment

To determine the reliability of the classified maps from our OBIA, on-screen assessments were performed for each site. One hundred points per site (50 points per class) were randomly selected within the extent of the site and assigned to either the tree or nontree class based on the unclassified NAIP image and expert knowledge. These points were then compared to the classified thematic map. An error matrix was populated for each category by summing the totals from all sites within a regional category, followed by the calculation of producer's, user's, and overall accuracies, and a kappa statistic (Congalton 2001).

Statistical Analysis

To determine whether tree canopy cover and biomass estimates were different between the remotely-sensed data and ground-measured data, we used a paired *t* test. For each subplot, differences between measurement methods were calculated by subtracting ground measurements (considered to be correct) from remotely-sensed measurements. Mean differences for each region (western juniper, Utah juniper, and mixed community) and tree canopy cover category (< 20%, 20–40%, and > 40%) were compared, using one-way ANOVA and the Tukey-Kramer honestly significant difference multiple comparison method. The correlation coefficient (*r*) was used to assess the relationship between remotely-sensed and ground-measured data. Statistical analysis in this study is used to assess the differences between ground measurements and remotely-sensed measurements at the subplot scale and should be used conservatively, as the actual tree canopy cover and aboveground biomass are unknown.

RESULTS

Tree Canopy Cover

Our OBIA classification method using NAIP imagery did not consistently underestimate or overestimate P-J canopy cover when compared to ground measurements (Fig. 2). Remotely-sensed and ground-measured tree canopy cover estimates were also highly correlated for each regional category (Fig. 2). For western juniper sites, correlation coefficients (*r*) quantifying the association between the two methods for estimating tree canopy cover ranged from 0.81 ($P < 0.01$; df 34) at Bridge Creek to 0.93 ($P < 0.01$; df 37) at Blue Mountain. For Onaqui

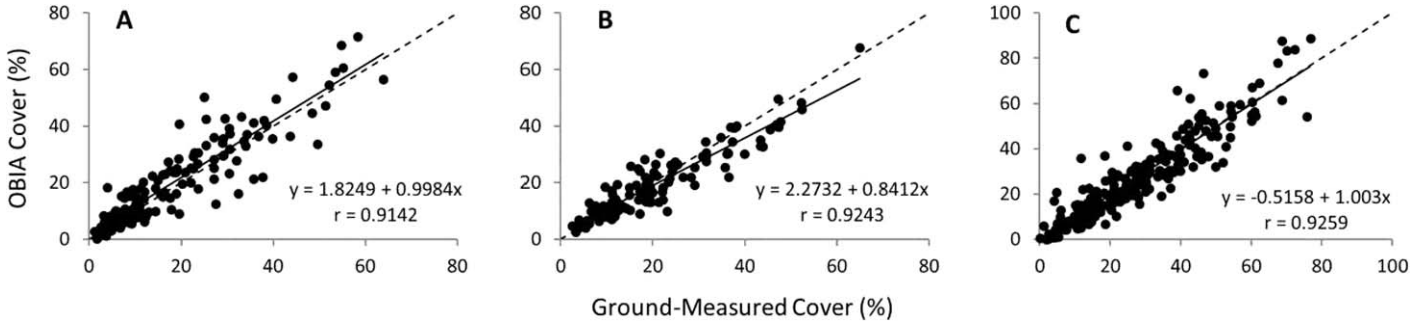

Figure 2. Regression of percent tree canopy cover estimates from ground-measured (*x*-axis) and object-based image analysis (OBIA; *y*-axis) cover by category. (**A**) JUOC sites (western juniper, $N=144$ subplots, $P<0.01$), (**B**) JUOS sites (Utah juniper, $N=112$, $P<0.01$), and (**C**) mixed community sites (comprised of either singleleaf piñon or twoneedle piñon with Utah juniper, $N=231$, $P<0.01$). A 1:1 dashed line is shown to aid comparison.

and Stansbury (Utah juniper sites) correlation coefficients were 0.85 ($P<0.01$; df 55) and 0.92 ($P<0.01$; df 55), respectively. The mixed community sites had the highest correlation coefficients ranging from 0.90 ($P<0.01$; df 33) at Marking Corral to 0.96 ($P<0.01$; df 43) at Scipio.

Although remotely-sensed P-J tree canopy cover estimates were not consistently higher or lower than ground-measured P-J canopy cover, differences between methods for regional categories were observed. On average, remotely-sensed tree canopy cover underestimated cover when compared to ground measurements on Utah juniper and mixed community sites, and overestimated cover when compared to ground measurements on western juniper sites (Table 2). When comparing remotely-sensed and ground measurements using the paired *t* test, western and Utah juniper sites were significantly different between the two methods ($P<0.05$; Table 2), while the mixed community was not ($P=0.3421$). For Utah juniper sites, differences between methods occurred mainly when tree canopy cover was greater than 20%. When tree canopy cover was between 20–40% on a subplot, remotely-sensed canopy cover measurements underestimated tree canopy cover by an average of 3% when compared to ground measurements ($P=0.0074$). When tree cover was greater than 40% on a subplot, remotely-sensed canopy cover measurements underestimated tree cover by an average of 6% when compared to ground measurements ($P=0.0023$). With the exception of Walker Butte, remotely-sensed tree canopy cover was typically overestimated for western juniper sites when compared to ground measurements. For subplots with tree cover between 20% and 40%, remotely-sensed cover was on average 3% greater than ground measurements. For subplots with tree cover greater than 40%, remotely-sensed cover was on average 4% greater than ground measurements.

Five sites (Blue Mountain, Devine Ridge, Marking Corral, Onaqui, and Stansbury; 57 total subplots), had both high-resolution and NAIP imagery for the comparison in spatial resolution. Canopy cover estimates yielded by high-resolution imagery and NAIP imagery were not significantly different ($P=0.8573$; Fig. 3). For tree canopy cover, the high-resolution imagery measurements overestimated tree canopy cover compared to ground measurements by an average of 1% across all subplots (range of differences –15.4% to 12.0%). Tree canopy cover from NAIP imagery measurements underestimated cover compared to ground measurements by an average of 1% across all subplots (range of differences –15.9% to 18.6%).

Across all regional categories, the average overall accuracy for the classified thematic maps was 91%, with an average kappa statistic of 0.81 (Table 3) indicating a strong agreement between the OBIA classification and reference data (Landis and Koch 1977). The nontree class was most often misclassified. For the Utah juniper sites, seven objects classified as trees were antelope bitterbrush patches found at the Stansbury site, and

Table 2. (A) Summary statistics for the object-based image analysis (OBIA) and ground-measured (Gnd) sampling methods for three categories: (1) JUOC sites (western juniper, $N=144$); (2) JUOS sites (Utah juniper, $N=112$); and (3) mixed community sites (comprised of either singleleaf piñon or twoneedle piñon with Utah juniper, $N=231$). (B) Comparison statistics of percent cover estimates from OBIA and Gnd data, using a paired *t* test. (C) Comparison statistics between categories average mean difference. Differences were calculated by subtracting Gnd from OBIA measurements.[1]

(A)				(B)		(C)		
Category	Method	Mean (% cover) (SE)	Range of tree canopy cover (%)	Category	*P* value	Category	Average mean difference (% cover) (SE)	Range of subplot differences (% cover)
JUOC	Gnd	18.19 (1.28)	1.1–63.8	JUOC	0.0009*	JUOC	1.80[a] (0.53)	−14.3 to 10.8
	OBIA	19.99 (1.36)	0.1–71.6	JUOS	0.0163*	JUOS	−1.13[b] (0.6)	−21.4 to 27.0
JUOS	Gnd	21.44 (1.45)	2.5–64.9	Mixed	0.3424	Mixed	−0.44[b] (0.42)	−16.1 to 25.4
	OBIA	20.31 (1.54)	2.6–67.8	—	—	—	—	—
Mixed	Gnd	26.64 (1.01)	0.1–76.7	—	—	—	—	—
	OBIA	26.2 (1.07)	0.0–88.8	—	—	—	—	—

[1]SE indicates standard error. Asterisks indicate significant difference between ground and remotely-sensed measurements, using the paired *t* test. Average mean differences with different letters are significantly different ($P<0.05$) from the other categories, using the Tukey-Kramer honestly significant difference multiple comparison procedure.

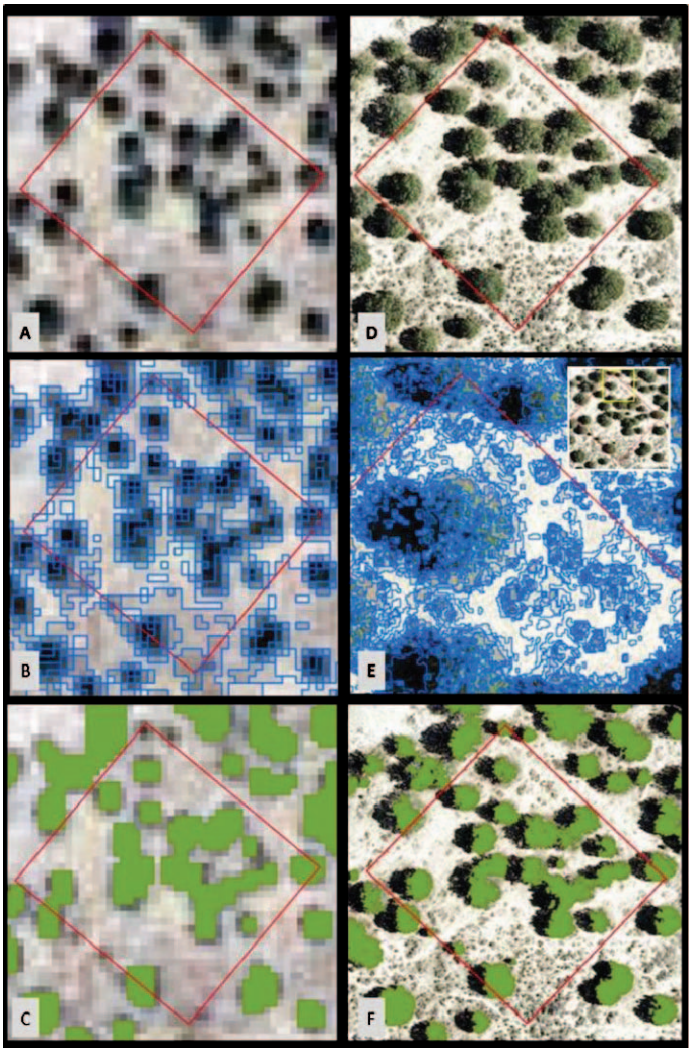

Figure 3. An example of (**A**) NAIP red, green, blue (RGB) image (1-m pixel resolution) and (**D**) high-resolution RGB image (HRI; 0.06-m pixel resolution). Red border is an example of one 30 × 33-m subplot. (**B**-NAIP) and (**E**-HRI) are examples of segmentation algorithms (multi-resolution followed by spectral difference) creating image objects (blue borders) for classification; (**C**-NAIP) and (**F**-HRI) are examples of the tree canopy cover classification, using object-based image analysis techniques. Ground measurements, NAIP, and HRI tree canopy cover measurements for the subplot shown were 24.8%, 27.4%, and 27.7%, respectively.

six objects were shadows. For the western juniper and mixed community sites, the majority of the misclassified objects were shadows (40 objects), or curl-leaf mountain mahogany (16 objects) found at Spruce Mountain, Blue Mountain, and Devine Ridge. Objects most often misclassified in the tree class were areas around the perimeter of a tree canopy that were classified as nontree (38 objects), or shadows obviously within the tree canopy area (19 objects). These misclassifications for the tree class could be found at all sites within the study area.

Aboveground Biomass

As with other studies, the relationship between ground-measured tree canopy cover and ground-measured aboveground biomass was strong for all regional categories. Ground-measured tree canopy cover explained 95% of the variability in aboveground biomass for western juniper sites ($P < 0.01$; df 143), 98% of the variability for Utah juniper sites ($P < 0.01$; df 111), and 96% for the mixed community sites ($P < 0.01$; df 230). When predicting P-J aboveground biomass, using remotely-sensed tree canopy cover, our method was not consistently higher or lower than ground-measured aboveground biomass. Additionally, there were high degrees of correlation between the ground measurements and predicted remotely-sensed estimates for each regional category (Fig. 4). For western juniper sites, correlation coefficients ranged from 0.78 ($P < 0.01$; df 34) at Bridge Creek to 0.90 ($P < 0.01$; df 37) at Blue Mountain. For the Utah juniper sites (Onaqui and Stansbury), correlation coefficients were 0.82 ($P < 0.01$; df 55) and 0.92 ($P < 0.01$; df 55), respectively. For the mixed community sites, correlation coefficients ranged from 0.85 ($P < 0.01$; df 36) at Spruce Mountain to 0.95 ($P < 0.01$; df 47) at Greenville Bench.

Table 3. Error matrix comparing object-based image analysis classification accuracies of cover classes (tree and nontree) for (A) western juniper, (B) Utah juniper, and (C) mixed community categories.[1]

Classified data	Trees	Nontree	Row total	User's accuracy
(A) Western juniper				
Tree	**176**	24	200	88%
Nontree	18	**182**	200	91%
Column total	194	206	—	—
Producer's accuracy	91%	88%	—	—
Overall accuracy: 90% kappa statistic: 0.79; $N = 400$				
(B) Utah juniper				
Tree	**91**	9	100	91%
Nontree	4	**96**	100	96%
Column total	95	105	—	—
Producer's accuracy	96%	91%	—	—
Overall accuracy: 94% kappa statistic: 0.87; $N = 200$				
(C) Mixed community				
Tree	**268**	32	300	89%
Nontree	35	**265**	300	88%
Column total	303	297	—	—
Producer's accuracy	88%	89%	—	—
Overall accuracy: 89% kappa statistic: 0.78; $N = 600$				

[1] N indicates number of points evaluated. Bold values indicate correct number of points classifed within the cover class.

As with the tree canopy cover estimates between the two methods, differences between ground-measured and predicted (remotely-sensed) aboveground biomass were significant ($P < 0.05$) for western and Utah juniper sites (Table 4). When analyzing individual sites within the western juniper category, no sites had significant differences between methods ($P > 0.05$). However, for western juniper subplots where tree canopy cover was less than 20%, there were significant differences between predicted and ground-measured aboveground biomass ($P = 0.0002$); predicted aboveground biomass was on average 16% (1713 $kg \cdot ha^{-1}$) greater than ground-measured aboveground biomass. When tree canopy cover was greater than 20%, predicted aboveground biomass was on average 3% (1 218 $kg \cdot ha^{-1}$) greater than ground-measured aboveground biomass ($P > 0.05$). For the Utah juniper sites, Stansbury's

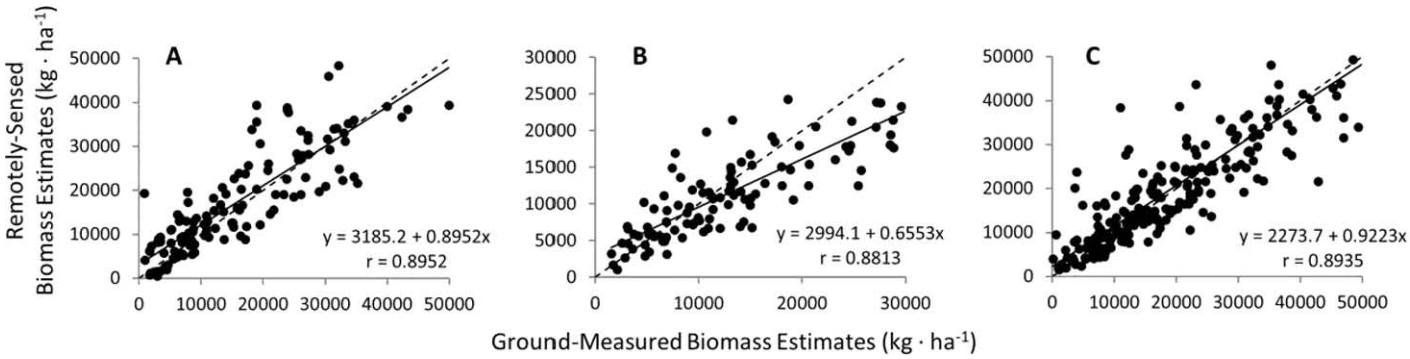

Figure 4. Regression of ground-measured aboveground biomass estimates (*x*-axis) and predicted aboveground biomass estimates from remotely-sensed measurements (*y*-axis) by category. (**A**) JUOC sites (western juniper, $N=144$ subplots, $P<0.01$), (**B**) JUOS sites (Utah juniper, $N=112$, $P<0.01$), and (**C**) mixed community sites (comprised of either singleleaf piñon or twoneedle piñon with Utah juniper, $N=231$, $P<0.01$). A 1:1 dashed line is shown to aid comparison.

predicted aboveground biomass was significantly different from ground-measured aboveground biomass ($P<0.0001$). For Stansbury subplots where tree canopy cover was greater than 20%, predicted aboveground biomass was on average 27% (7 540 kg · ha^{-1}) less than ground-measured aboveground biomass ($P<0.0001$). Where tree canopy cover was less than 20%, predicted aboveground biomass was on average 10% (838 kg · ha^{-1}) less than ground-measured aboveground biomass ($P=0.2639$).

DISCUSSION

Results from this study support using OBIA methods and NAIP imagery to monitor and assess P-J canopy cover and aboveground biomass across the Great Basin. Although differences between remotely-sensed and ground measurements occurred, there was a high degree of correlation for both tree canopy cover and aboveground biomass. Differences in tree canopy cover were minimal between OBIA and ground measurements (± 2% on average across all regional categories), and remotely-sensed predicted aboveground biomass on average was within ± 2% (43 kg · ha^{-1}) of ground-measured aboveground biomass. Although some accuracy and precision may be lost when utilizing aerial imagery to identify P-J canopy cover and aboveground biomass, it is still a good alternative to both time-consuming and expensive ground monitoring and inventory practices.

NAIP imagery was selected for this study because the spatial resolution (0.5 m to 0.1 m pixels) was adequate for extracting P-J trees, the spatial coverage was complete for all study sites, and the postprocessed (orthorectified) images were available free of charge. Correlation between ground and remotely-sensed measurements are highly dependent on the spatial resolution of the imagery and the relative size of the object or plant of interest (Jensen 2005; Karl et al. 2012; Mirik and Ansley 2012). For our study, the average longest tree diameter and perpendicular tree diameter for western juniper were 2.8 m for both measurements, for Utah juniper they were 2.5 and 2.4 m, for twoneedle piñon they were 2.2 and 2.1 m, and for singleleaf piñon they were 2.1 and 2.0 m, respectively. Because of the size of the objects (P-J trees) to be extracted, we saw little to no differences between the NAIP and high-resolution imagery for estimating tree canopy cover. Species identification between piñon and juniper tree species was not evaluated using NAIP imagery in our study. In agreement with Browning et al. (2009), species identification is not easily achieved with coarse (greater than 1-m pixel resolution) imagery; however, Hulet et

Table 4. (A) Summary statistics for ground-measured (Gnd) and predicted (Pred) P-J aboveground biomass for three categories: (1) JUOC sites (western juniper, $N=144$); (2) JUOS sites (Utah juniper, $N=112$); and (3) mixed community sites (comprised of either singleleaf piñon or twoneedle piñon with Utah juniper, $N=231$). (B) Comparison statistics of aboveground biomass estimates between Gnd and Pred data, using a paired *t* test. (C) Comparison statistics between categories average mean difference. Differences were calculated by subtracting Gnd from Pred measurements.[1]

(A)				(B)		(C)		
Category	Method	Mean (kg · ha^{-1}) (SE)	Range of biomass estimates (kg · ha^{-1})	Category	*P* value	Category	Average mean difference (kg · ha^{-1}) (SE)	Range (kg/ha) and percent of subplot differences
JUOC	Gnd	17 276 (1 194)	792–66 126	JUOC	0.0109*	JUOC	1 375[a] (560)	−24 426 (44%)–20 543 (52%)
	Pred	18 650 (1 190)	575–64 035	JUOS	< 0.0001*	JUOS	−2 074[b] (635)	−7 059 (51%)–9 272 (55%)
JUOS	Gnd	14 705 (1 354)	1 545–40 360	Mixed	0.2548	Mixed	575[a] (442)	−23 845 (47%)–16 751 (58%)
	Pred	12 631 (1 349)	1 085–41 913	—	—	—	—	—
Mixed	Gnd	21 879 (943)	930–83 112	—	—	—	—	—
	Pred	22 451 (940)	1 655–89 829	—	—	—	—	—

[1]SE indicates standard error. Asterisks indicate significant difference between ground and predicted measurements, using the paired *t* test. Average mean differences with different letters are significantly different ($P<0.05$) from the other categories, using the Tukey-Kramer honestly significant difference multiple comparison procedure. Range of subplot differences is followed by the percentage of total biomass difference.

al. (2013) did successfully distinguish species with the use of fine (0.06-m pixel resolution) imagery.

Although NAIP imagery was sufficient to extract tree canopy cover within an acceptable error rate (± 5%), it should be noted that small trees (diameter < 1 m) were likely missed during the classification process. A failure to account for smaller trees may influence identifying initial encroachment and infilling patterns across a landscape, but is unlikely to have a major influence on remotely-sensed aboveground biomass estimates at a broad scale. In this study, we found that predicted remotely-sensed aboveground biomass estimates for subplots with tree canopy cover less than 20%, between 20% and 40%, and greater than 40%, were on average 13% greater (1 220 $kg \cdot ha^{-1}$), 4% less (850 $kg \cdot ha^{-1}$), and 2% less (1 009 $kg \cdot ha^{-1}$) than ground-measured aboveground biomass, respectively. Remotely-sensed tree canopy cover for the Utah juniper and mixed communities was on average less than ground measurements, particularly as tree canopy cover increased. For western juniper sites, remotely-sensed tree canopy cover was on average greater than ground measurements as cover increased. These patterns likely reduced the overall average differences between predicted and ground-measured aboveground biomass for P-J woodlands when tree canopy cover was greater than 20%. When tree canopy cover was less than 20%, remotely-sensed tree canopy cover was on average 6% greater than ground-measured tree canopy cover across all sites providing one possible explanation for the differences observed between predicted and ground-measured aboveground biomass for P-J woodlands. These results suggest that predicted aboveground biomass with the use of remotely-sensed tree canopy cover is highly dependent on the user's ability to extract tree canopy cover from the imagery source, particularly for P-J woodland with < 20 or > 40% tree canopy cover.

Sources of error that influence the user's ability to extract tree canopy cover that should be considered when utilizing aerial imagery to identify P-J woodland tree canopy cover include shadows, terrain effects, quality of imagery (spatial, spectral, and radiometric resolution), and incorrect orthorectification of measurement subplots (Fensham et al. 2002; Jensen 2005; Browning et al. 2009; Moffet 2009). For this study where we primarily dealt with P-J species, seasonal variations or the collection period of NAIP imagery was of less concern. However, background interference from shrubs (i.e., antelope bitterbrush or curl-leaf mountain mahogany) did influence the overall classification of tree canopy cover. Shrubs that were classified as trees erroneously increased total tree canopy cover, which, in turn, likely overestimated P-J aboveground biomass. For this study, OBIA rule sets were developed on a site-by-site basis that included a range of P-J canopy cover within each site. P-J woodlands with < 20% tree canopy cover (i.e., greater amounts of understory vegetation), may require separate OBIA rule sets to better account for understory vegetation and minimize the misclassification of nontree classes.

The classification of P-J species was also influenced by shadows. A method to mitigate shadow effects for near-earth imagery through the use of high dynamic range nadir images has been presented (Cox and Booth 2009); however, the feasibility of the method for aerial imagery is limited. For this study, shadow effects were mitigated through the use of spectral and spatial features found within the OBIA rule sets. The spatial features incorporated within the OBIA rule set allowed us to account for various amounts of shadows (2–16%) found within the aerial imagery by growing or shrinking objects based on neighboring image objects on a site-by-site basis.

Inaccuracies between ground measurements and OBIA estimates were also likely due to data collection methods. All trees with the base of the trunk within the subplot were included in the ground measurements. However, with the use of planimetric imagery it was difficult to determine if trees around the perimeter of the subplot were actually within the subplot boundaries. Errors also likely occurred because of discrepancies between the horizontal error associated with NAIP imagery (± 6 m) and our subplot placements, which used a Trimble GPS with submeter accuracy. Additionally, remotely-sensed tree canopy cover measurements may have been affected by tree clustering, or an overlap of branches between neighboring trees, which would have contributed to the underestimation of tree canopy cover compared to ground measurements. Tree clustering was minimal in the study for all sites, with a few exceptions where a subplot tree canopy cover was > 40%. Vegetation and imagery anomalies found within a site (e.g., tree clustering, shadows) may require multiple OBIA rule sets per site to increase the accuracy of the remotely-sensed tree canopy cover estimates.

MANAGEMENT IMPLICATIONS

Object-based image analysis methods combined with NAIP imagery can provide land managers with quantitative data that can be used to evaluate P-J woodlands rapidly at a scale necessary to make management decisions. Training subplots (approximately 20% of the total ground-measured subplots) were successfully used to develop OBIA rule sets that were then tested over larger extents. This suggests that land managers could potentially reduce the number of ground-measured subplots across an area of interest, and utilize OBIA methods and NAIP imagery to extend monitoring practices. Depending on site characteristics and image quality, ground-measured subplots could systematically be placed throughout an area of interest to capture the variation found on a specific site, and then used to develop OBIA rule sets. Rule sets could then be used to quantify large land areas rapidly and inexpensively, within reason. It should be noted that validation subplots will need to be included to assess the overall accuracy of the classification, and that multiple OBIA rule sets may be needed to better estimate P-J canopy cover, depending on the stage of woodland succession (Miller et al. 2005) and dominant understory vegetation across a landscape.

P-J canopy cover data derived from these processes, coupled with geospatial data layers (Johnson and Miller 2006; Weisberg et al. 2007; Davies et al. 2010), provide managers with tools to aid in planning and prioritizing management practices (Mirik and Ansley 2012), analyzing fire behavior and assessing fire suppression strategies (Arroyo et al. 2008), and managing habitats on broad spatial scales. Because NAIP imagery is regularly collected and affordable, baseline measurements of P-J woodland canopy cover may be evaluated and temporal

changes monitored through various disturbances and climate regimes.

ACKNOWLEDGMENTS

We are grateful to Jim McIver and Dustin Johnson for reviewing earlier versions of this manuscript. As well as Brad Jessop, Jaime Ratchford, and Travis Miller for substantial field support. We also appreciate the reviews by the anonymous reviewers and Associate Editor. This is Contribution Number 17 of the Sagebrush Steppe Treatment Evaluation Project (SageSTEP); funding was provided by the US Joint Fire Science Program, the Bureau of Land Management, the National Interagency Fire Center, the Great Northern Landscape Conservation Cooperative, and Brigham Young University.

LITERATURE CITED

Anderson, J. J., and N. S. Cobb. 2004. Tree cover discrimination in panchromatic aerial imagery of pinyon–juniper woodlands. *Photogrammetric Engineering & Remote Sensing* 70:1063–1068.

Ansley, R. J., M. Mirik, B. W. Surber, and S. C. Park. 2012. Canopy area and aboveground mass of individual redberry juniper (*Juniperus pinchotii*) trees. *Rangeland Ecology & Management* 65:189–195.

Arroyo, L. A., C. Pascual, and J. A. Manzanera. 2008. Fire models and methods to map fuel types: the role of remote sensing. *Forest Ecology and Management* 6:1239–1252.

Baatz, M., and A. Schäpe. 2000. Multiresolution segmentation—an optimization approach for high quality multi-scale image segmentation. *In:* J. Strobl et al. [eds.]. *Angewandte Geographische Informationsverarbeitung XII*. Heidelberg, Germany: Wichmann. p. 12–23.

Bates, J. D., R. F. Miller, and T. Svejcar. 2005. Long-term successional trends following western juniper cutting. *Rangeland Ecology & Management* 58:533–541.

Blaschke, T. 2010. Object based image analysis for remote sensing. *ISPRS Journal of Photogrammetry and Remote Sensing* 65:2–16.

Browning, D. M., S. R. Archer, and A. T. Byrne. 2009. Field validation of 1930s aerial photography: what are we missing? *Journal of Arid Environments* 73:844–853.

Chuvieco, E., I. Aguado, M. Yebra, H. Nieto, J. Salas, M. P. Martin, L. Vilar, J. Martinez, S. Martin, P. Ibaraa, J. de la Riva, J. Baeza, F. Rodriguez, J. R. Molina, M. A. Herrera, and R. Zamora. 2010. Development of a framework for fire risk assessment using remote sensing and geographic information system technologies. *Ecological Modelling* 221:46–58.

Congalton, R. G. 2001. Accuracy assessment and validation of remotely sensed and other spatial information. *International Journal of Wildland Fire* 10:321–328.

Cox, S. E., and D. T. Booth. 2009. Shadow attenuation with high dynamic range images. *Environmental Monitoring and Assessment* 158:231–241.

Davies, K. W., S. L. Petersen, D. D. Johnson, D. B. Davis, M. D. Madsen, D. L. Zvirzdin, and J. D. Bates. 2010. Estimating juniper cover from national agriculture imagery program (NAIP) imagery and evaluating relationships between potential cover and environmental variables. *Rangeland Ecology & Management* 63:630–637.

Fensham, R. J., R. J. Fairfax, J. E. Holman, and P. J. Whitehead. 2002. Quantitative assessment of vegetation structural attributes from aerial photography. *International Journal of Remote Sensing* 23:2293–2317.

Huang, C., G. P. Asner, R. E. Martin, N. N. Barger, and J. C. Neff. 2009. Multiscale analysis of tree cover and aboveground carbon stocks in pinyon-juniper woodlands. *Ecological Applications* 19:668–681.

Hulet, A., B. A. Roundy, S. L. Petersen, R. R. Jensen, and S. C. Bunting. 2013. Assessing the relationship between ground measurements and object-based image analysis of land cover classes in pinyon and juniper woodlands. *Photogrammetric Engineering & Remote Sensing* 79:799–808.

Hulet, A., B. A. Roundy, S. L. Petersen, R. R. Jensen, and S. C. Bunting. 2014. Cover estimations using object-based image analysis techniques across multiple scales in pinyon and juniper woodlands. *Rangeland Ecology & Management* 67:318–327.

Jensen, J. R. 2005. Introductory digital image processing: a remote sensing perspective. Upper Saddle River, NJ, USA: Pearson Prentice Hall. 526 p.

Johnson, D. D., and R. F. Miller. 2006. Structure and development of expanding western juniper woodlands as influenced by two topographic variables. *Forest Ecology and Management* 229:7–15.

Karl, J. W., M. C. Duniway, S. M. Nusser, J. D. Opsomer, and R. S. Unnasch. 2012. Using very-large scale aerial imagery for rangeland monitoring and assessment: some statistical considerations. *Rangeland Ecology & Management* 65:330–339.

Ko, D., N. Bristow, D. Greenwood, and P. Weisberg. 2009. Canopy cover estimation in semiarid woodlands: comparison of field-based and remote sensing methods. *Forest Science* 55:132–141.

Landis, J., and G. Koch. 1977. The measurement of observer agreement for categorical data. *Biometrics* 33:159–174.

Madsen, M. D., D. L. Zvirzdin, B. D. Davis, S. L. Petersen, and B. A. Roundy. 2011. Feature extraction techniques for measuring piñon and juniper tree cover and density, and comparison with field-based management surveys. *Environmental Management* 47:766–776.

McGinnis, T. W., C. D. Shook, and J. E. Keeley. 2010. Estimating aboveground biomass for broadleaf woody plants and young conifers in Sierra Nevada, California, forests. *Western Journal of Applied Forestry* 25:203–209.

McIver, J., and M. Brunson. 2014. Multidisciplinary, multisite evaluation of alternative sagebrush steppe restoration treatments: the SageSTEP project. *Rangeland Ecology & Management* 67:435–439.

McIver, J. D., M. Brunson, S. Bunting, J. Chambers, N. Devoe, P. Doescher, J. Grace, D. Johnson, S. Knick, R. Miller, M. Pellant, F. Pierson, D. Pyke, K. Rollins, B. Roundy, E. Schupp, R. Tausch, and D. Turner. 2010. The Sagebrush Steppe Treatment Evaluation Project (SageSTEP): a test of state-and transition theory. Fort Collins, CO, USA: US Department of Agriculture Forest Service, Rocky Mountain Research Station. Report RMRS-GTR-237.

Meneguzzo, D. M., G. C. Liknes, and M. D. Nelson. 2013. Mapping trees outside forests using high-resolution aerial imagery: a comparison of pixel- and object-based classification approaches. *Environmental Monitoring and Assessment* 185:6261–6275.

Miller, E. L., R. O. Meeuwig, and J. D. Budy. 1981. Biomass of singleleaf pinyon and Utah Juniper. Ogden, UT, USA: US Department of Agriculture, Forest Service, Intermountain Forest and Range Experimental Station, Research Paper INT-273. 18 p.

Miller, R. F., J. D. Bates, T. J. Svejcar, F. B. Pierson, and L. E. Eddleman. 2005. Biology, ecology, and management of western juniper. Corvallis, OR, USA: Oregon State University, Technical Bulletin 152. 77 p.

Miller, R. F., J. Ratchford, B. A. Roundy, R. J. Tausch, C. Pereia, A. Hulet, and J. Chambers. 2014. Response to conifer encroached shrublands in the Great Basin to prescribed fire and mechanical treatments. *Rangeland Ecology & Management* 67:468–481.

Miller, R. F., T. J. Svejcar, and J. A. Rose. 2000. Impacts of western juniper on plant community composition and structure. *Journal of Range Management* 53:574–585.

Miller, R. F., and R. J. Tausch. 2001. The role of fire in pinyon and juniper woodlands: a descriptive analysis. *In:* K. E. M. Galley and T. P. Wilson [eds.]. Proceedings of the Invasive Species Workshop: the Role of Fire in the Control and Spread of Invasive Species. Fire Conference 2000: the First National Congress on Fire Ecology, Prevention, and Management. Miscellaneous Publication No. 11, Tall Timber Research Station, Tallahassee, FL, USA. p. 15–30.

Mirik, M., and R. J. Ansley. 2012. Comparison of ground-measured and image-classified mesquite (*Prosopis glandulosa*) canopy cover. *Rangeland Ecology & Management* 65:85–95.

Moffet, C. A. 2009. Agreement between measurements of shrub cover using ground-based methods and very large scale aerial imagery. *Rangeland Ecology & Management* 62:268–277.

Pierson, F. B., C. J. Williams, P. R. Kormos, S. P. Hardegree, P. E. Clark, and B. M. Rau. 2010. Hydrologic vulnerability of sagebrush steppe following pinyon and juniper encroachment. *Rangeland Ecology & Management* 63:614–629.

Platt, R.V., and L. Rapoza. 2008. An evaluation of an object-oriented paradigm for land use/land cover classification. *The Professional Geographer* 60:87–100.

Roundy, B. A., R. F. Miller, R. J. Tausch, K. Young, A. Hulet, B. Rau, B. Jessop, J. C. Chambers, and D. Egget. 2014a. Understory cover responses to piñon-juniper treatments across tree cover gradients in the Great Basin. *Rangeland Ecology & Management* 67:482–494.

Roundy, B. A., K. Young, N. Cline, A. Hulet, R. F. Miller, R. J. Tausch, and B. Rau. 2014b. Piñon-juniper reduction increases soil water availability of the resource growth pool. *Rangeland Ecology & Management* 67:495–505.

Sabin, B. S. 2008. Relationship between allometric variables and biomass in western juniper *(Juniperus occidentalis*) [thesis]. Corvallis, OR, USA: Oregon State University. 129 p.

Sankey, T., and N. Glenn. 2011. Landsat-5 TM and lidar fusion for sub-pixel juniper tree cover estimates in a western rangeland. *Photogrammetric Engineering & Remote Sensing* 77:1241–1248.

Sankey, T., R. Shrestha, J. B. Sankey, S. Hardegree, and E. Strand. 2013. Lidar-derived estimate and uncertainty of carbon sink in successional phases of woody encroachment. *Journal of Geophysical Research: Biogeosciences* 118:1144–1155.

Skog, K. E., R. Rummer, B. Jenkins, N. Parker, P. Tittmann, Q. Hart, R. Nelson, E. Gray, A Schmidt, M. Patton-Mallory, and G. Gordon. 2009. A strategic assessment of biofuels development in the Western States. *In:* W. McWilliams, G. Moisen, and R. Czaplewski [comps.]. 2008 Forest Inventory and Analysis (FIA) Symposium. Fort Collins, CO, USA: US Department of Agriculture, Forest Service. Report RMRS-P-56. p. 1–13.

Strand, E. K., L. A. Vierling, A. M. S. Smith, and S. C. Bunting. 2008. Net changes in aboveground woody carbon stock in western juniper woodlands, 1946–1998. *Journal of Geophysical Research* 113:G01013. doi:10.1029/2007JG000544.

Tausch, R. J. 2009. A structurally based analytic model for estimation of biomass and fuel loads of woodland trees. *Natural Resource Modeling* 22:463–488.

Tausch, R. J., and P. T. Tueller. 1990. Foliage biomass and cover relationships between tree- and shrub-dominated communities in pinyon-juniper woodlands. *Great Basin Naturalist* 50:121–134.

Trimble. 2011. eCognition Developer 8.64.1 reference book, version 8.64.1. München, Germany: Trimble Germany GmbH.

Weisberg, P. J., E. Lingua, and R. B. Pillai. 2007. Spatial patterns in pinyon-juniper woodland expansion in central Nevada. *Rangeland Ecology & Management* 60:115–124.